Experimental Studies of the Thermoelectric Properties of Microstructured and Nanostructured Lead Salts

by

Kathleen C. Barron

Submitted to the Department of Mechanical Engineering
in Partial Fulfillment of the Requirements for the Degree of
Bachelors of Science in Mechanical Engineering

at the
Massachusetts Institute of Technology
February 2005

Signature of Author .....
Department of Mechanical Engineering
January 14, 2005

Certified by .....
Gang Chen
Professor of Mechanical Engineering
Thesis Supervisor

Accepted by .....
Ernest Cravalho
Undergraduate Officer

Experimental Studies in the Thermoelectric Properties of Microstructured and Nanostructured Lead Salts

by

Kathleen C. Barron

Submitted to the Department of Mechanical Engineering
in Partial Fulfillment of the Requirements for the Degree of
Bachelors of Science in Mechanical Engineering

Abstract

Thermoelectric devices allow for direct conversion between thermal and electrical energy. There applications, however, are severely limited by their inefficiency. A reduction in thermal conductivity of a material potentially enhances its overall thermoelectric performance and can improve the efficiency of thermoelectric devices. Thermal conductivity can be reduced by boundary phonon scattering for materials in which the grain size is comparable to or less than the phonon mean free path. Samples of PbTe and PbSe were prepared by hot pressing nano-size and micro-sized particles and the thermal diffusivity, the Seebeck coefficient, and the electric conductivity of the samples were measured. The samples made from the nano-sized particles showed no reduction in thermal conductivity and no enhancement of thermoelectric properties. It is suspected that the grain growth occurred during the hot pressing stage, resulting in grains sizes larger than the original particle. The grains may have grown substantially larger than the phonon mean free path. Grains of this dimension are not effective at scattering phonons.

Thesis Supervisor: Gang Chen
Title: Professor of Mechanical Engineering

Acknowledgements

I would like to express my gratitude to Prof. Gang Chen for this wonderful opportunity and to Hohyun Lee for his support and his guidance through this project.

Contents

1.0 Introduction

In thermoelectric materials, electrical energy can be directly converted into thermal energy and thermal energy into electrical energy. Direct conversion between electrical and thermal energy is possible because of two important thermoelectric effects: the Seebeck effect and the Peltier effect. The Seebeck effect refers to the existence of an electric potential across a thermoelectric material subject to a temperature gradient. The Peltier effect refers to the absorption of heat into one end of a thermoelectric material and the release of heat from the opposite end due to a current flow through the material.

Thermoelectric materials are used in the construction of refrigerators and power generators. Direct conversion of thermal and electric energy means that the thermoelectric devices are often more reliable than traditional mechanic devices and suffer less wear. However, thermoelectric devices have a much lower efficiency than traditions devices. To raise the efficiency of these devices, materials with enhanced thermoelectric properties need to be found.

One method of increasing the thermoelectric performance of materials is to manufacture materials with a very fine grain structure. If the characteristic length scale of the grains in a polycrystalline material is comparable to or less than the phonon mean free path, approximately 200~300 nm, phonons will be scattered off the grain boundaries, leading to a reduction in the thermal conductivity. Since the thermoelectric performance of a material is inversely proportional to the thermal conductivity, lowering a material's thermal conductivity could enhance its thermoelectric performance.

The goal of this study is to compare the thermoelectric performance of fine grained PbTe and PbSe. The samples were made by hot pressing particles of thermoelectric materials. There were two sizes of particles that were used: nanometer-sized particles and micrometer-sized particles. The samples made from the nano-sized particles should have a finer grain structure than those produced from the micro-sized.

This thesis will first go into depth on the theoretic background behind the theory, explaining basic thermoelectric principals and how they can be applied to energy conversion devices. It will also cover recent developments in the field thermoelectrics, including the theory behind increased thermoelectric performance due to grain boundaries. The paper then will explore the detail of the actual experiment and examine the results. Finally, the results will be discussed and conclusions drawn.

2.0 Theoretical Background

The theories behind thermoelectric effects and possible methods for altering thermoelectric properties have been extensively studied over the years. These theories have led to great improvements in the performance of thermoelectric materials since research began and current theories predict even greater improvement in performance can be achieved.

2.1 Thermoelectric Properties

Pollock[1] in the *CRC Handbook of Thermoelectrics* provides a solid introduction to the basics of thermoelectric properties.

An isolated conductor, subject to a temperature gradient, will develop an electric potential between the two extreme temperatures. The generated voltage is due to the diffusion of charge carriers from the hot side of the conductor to the cold. The charge carriers will continue to move from the hot side to the cold until an electric potential of equal magnitude to the thermal potential is established. In n-type materials the change carriers are electrons, while in p-type materials the charge is carried by the movement of holes.

This effect is called the Seebeck effect after Thomas J. Seebeck, who first observed this behavior in 1823. The magnitude of the potential difference along the material, E_A, is proportional to the temperature difference, ΔT, between the two ends according to

$$E_A = S_A \Delta T \tag{1}$$

where S_A is the absolute Seebeck coefficient of the material.

In a closed circuit of two dissimilar conductors, as shown in Figure 1, the temperature difference between the two junctions will impose an electromagnetic force (emf) around the loop. The relationship between the induced emf, V, and the temperature difference is

$$V = S_{AB} \Delta T \tag{2}$$

where S_{AB} is the relative Seebeck coefficient, defined as

$$S_{AB} = S_A - S_B \ . \tag{3}$$

S_A and S_B are the absolute Seebeck coefficients of conductor A and conductor B, respectively.

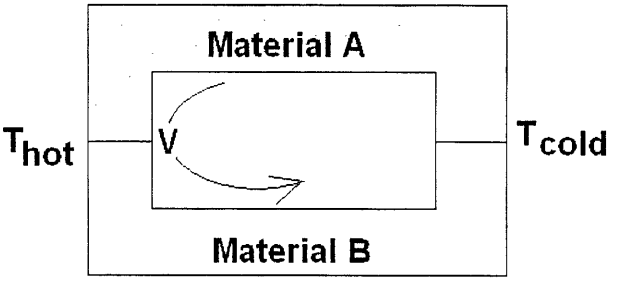

Figure 1: The Seebeck effect in a closed circuit of two dissimilar conductors. The temperature difference between the two junctions drives the voltage around the loop.

The Peltier effect is related to the ability of charge carriers to carry thermal energy as well as charge as they move through a conductor. The heat flow, Q_A, moving through a material is proportional to the electric current, I, according to

$$Q_A = \Pi_A I \tag{4}$$

where Π_A is the absolute Peltier coefficient of material A.

As a given current passes from one conductor to another, the amount of heat energy transported per unit current may either increase or decrease depending on the difference in absolute Peltier coefficients of the materials. Therefore, at the junction of a current-carrying circuit comprised of dissimilar conductors, heat is either absorbed or released in order to balance the heat flow into and out of the junction. Figure 2 shows a schematic of the Peltier effect in a closed circuit of conductor A and conductor B.

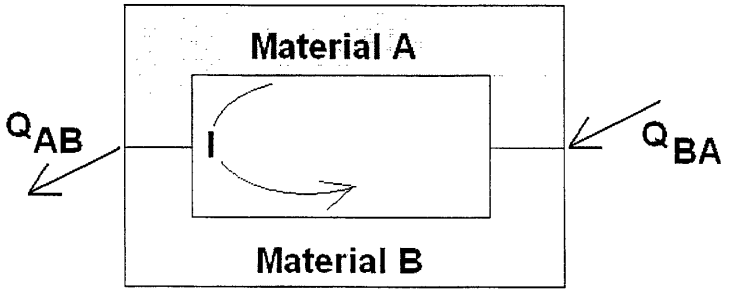

Figure 2: The Peltier effect in a closed circuit of two dissimilar conductors. As the current flows through the loop, heat is liberated from one junction and absorbed at the opposite. The heat liberated at one end, Q_{AB}, is equal in magnitude to the heat absorbed at the opposite, Q_{BA}.

The amount of heat released or generated at each junction is proportional to the current through the circuit according to

$$Q_{AB} = \Pi_{AB} I \tag{5}$$

where Π_{AB} is the relative Peltier coefficient. The relative Peltier coefficient is related to the absolute Peltier coefficients of both conductors as

$$\Pi_{AB} = \Pi_A - \Pi_B \tag{6}$$

The Thompson effect describes the process by which heat is absorbed or liberated by a homogeneous conductor, conducting a current through a temperature gradient. The heat flow per unit length of the conductor, Q_A/l, is related to the current and the temperature gradient as

$$Q_A/\ell = \beta_A I \frac{dT}{dx} \tag{7}$$

where β_A is the Thompson coefficient of conductor A.

Both the Peltier and the Thompson effects are thermodynamically reversible.

Consider a closed circuit of two dissimilar conductors with one junction in contact with a heat source and the other in contact with a heat sink, as shown in Figure 3. The heat sink maintains a temperature of T_0, and the heat source maintains a temperature of $T_0+\Delta T$.

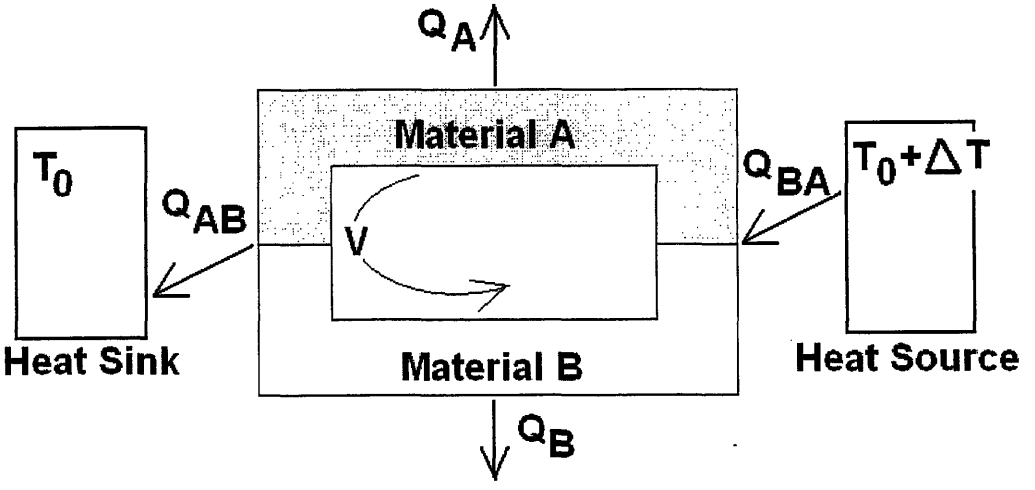

Figure 3: A reversible heat engine of two thermoelectric materials in a closed circuit in which all three thermoelectric effects are active. The circuit junctions are in contact with a heat sink and heat source, which provides the energy to maintain the temperature difference.

As a reversible heat engine, the thermal energies can be equated to the electrical work as

$$E_{AB}I = \Pi_{AB}(T_0 + \Delta T) + \Pi_{AB}(T_0) + \int_{T_0}^{T_0+\Delta T} \frac{\beta_A - \beta_B}{T} dT = 0 \qquad (8)$$

which can be simplified to

$$\frac{dE_{AB}}{dT} = \frac{d\Pi_{AB}}{dT} + (\beta_B - \beta_A) = S_{AB} \qquad (9)$$

Equation 9 gives the fundamental thermodynamic theorem for closed thermoelectric circuits.

There is a simple relationship between the Seebeck and Peltier coefficients,

$$\Pi_{AB} = S_{AB}T \qquad (10)$$

2.2 Application of Thermoelectric Materials

Since the thermoelectric properties directly relate the thermal and electrical states of a material, thermoelectric materials can be combined into devices capable of directly convert thermal energy into electrical energy or vise versa. Thermoelectric materials are used to construct thermoelectric refrigerator, heat pumps, and power generation devices. Since such devices require no moving parts, they do not suffer from wear and are highly reliable.

A simple thermoelectric cooler, such as the one pictured in Figure 4a, consists of two thermoelectric legs electrically connected in series. One of the legs is an n-type thermoelectric and the other is a p-type. If a driving voltage is applied, current will be force through the device. In the n-type leg, the current is carried by the diffusion of electrons in the opposite direction of the current flow. In the p-type leg, the current is carried by diffusion of holes in the direction of the current. Both the electrons in the n-type leg and the holes in the p-type leg carry thermal energy from the cold side to the hot side when current flows. Though the current is flowing through them in series, the thermal energy is being pumped away from the cold side to the hot in parallel.

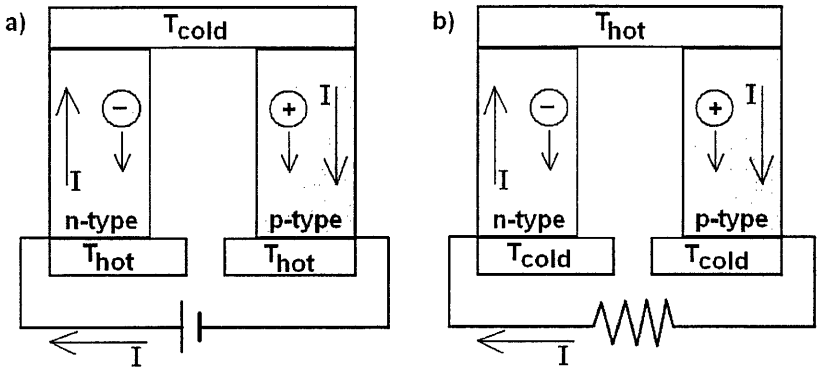

Figure 4: a) Schematic of a simple thermoelectric heater
b) Schematic of a simple thermoelectric heater. Current flow through resistor represents electric work produced.

The operation of a thermoelectric power generator, pictured in Figure 4b, is similar to that of the thermoelectric cooler run in reverse. Rather than using a driving voltage to pump heat and establish a temperature difference, the power generator uses an existing temperature difference to produce electrical power. Electrons in the n-type leg and holes in the p-type leg will diffuse from the hot side to the cold, creating a current around the loop. This current can be used to perform useful work.

Actual thermoelectric devices consist of an array of p-type and n-type leg pairs arranged so that the electric current will flow through all the legs in series and the heat will flow through all in parallel.

Thermoelectric materials are also used in the construction of thermocouples. Thermocouples consist on two long thermoelectric leads joined in series. Usually one of which is n-type and the other of which is p-type. When the junction of the two leads is put in contact with an object of higher or lower temperature, a temperature difference will be established between the junction and the far ends of the leads. The far ends are assumed to be at the same temperature as the ambient temperature of the room. Since the leads are of thermoelectric materials, the temperature difference will lead to a voltage difference by the Seebeck effect. By measuring the voltage difference between the two leads, the temperature difference can be calculated if the Seebeck coefficient of both legs is known.

2.3 Figure of Merit

For thermoelectric coolers and power generator to be practical and competitive with more traditional forms of technology, the thermoelectric devices must reach a comparable level of efficiency at converting between thermal and electric energy. The total efficiency of the device will naturally be related to a combination of the thermoelectric properties of both the p-type and the n-type legs.

In thermoelectric materials research, however, it is more convenient to look at the thermoelectric performance of each material singularly, rather than as a component within a device. A single material Figure of Merit has defined as

$$Z = \frac{S^2\sigma}{k} \tag{11}$$

where σ is the material's electrical conductivity and k its thermal conductivity. The Z factor provides a means of comparing overall thermoelectric performance between materials. The thermoelectric Figure of Merit has the units of the K^{-1} so often it is multiplied by the mean absolute operating temperature to give the dimensionless figure ZT.

Currently, the best available thermoelectric materials exhibit a ZT near unity at their operating temperatures. To achieve viable efficiencies for thermoelectric devices, the materials used should have much higher ZTs. For example, a thermoelectric cooler with the same efficiency of that of a Freon cooler would need to be constructed with thermoelectric material with ZTs of three to four[2]. To increase ZT, expressed as $S^2\sigma$, also known as the power factor, needs to be increased in relation to the thermal conductivity.

2.4 Efforts to Increase ZT

Most efforts to increase ZT have centered about finding a way to decrease the thermal conductivity. The thermal conductivity of any solid is a sum of the thermal conductivity of the lattice, k_l, due to phonon transport, and the electric thermal conductivity, k_e, due to the transport of charge carriers. Most thermoelectric materials are also semiconductors, however. For many semiconductor materials, the electric thermal conductivity, which is directly proportional to the electric conductivity, is a substantial portion of the overall thermal conductivity.

Though the thermal and electric conductivity are not entirely independent, the ratio of thermal to electric conductivity can still be decreased by scattering the phonons responsible for heat transport through the lattice. Phonon scattering can be achieved without altering the ability of the electrons to pass through, thereby lowering the σ/k ratio.

Both theoretical and experimental research is exploring phonon scattering as an effective method of reducing the thermal conductivity of thermoelectric materials, and thereby increasing ZT. Research is ongoing to increase thermoelectric performance in bulk materials. In addition, nanostructrured materials have been found to have increased thermoelectric performance compared to their bulk alloys.

2.4.1 Bulk Materials

Extensive theoretical modeling of the thermoelectric properties of bulk materials has been performed base off of the Boltzmann's equation under the assumption of constant relaxation time.[3] Under this model, ZT depends only on the electron effective mass, the

carrier mobility, the phonon thermal conductivity, and the reduced chemical potential, which is controllable by doping.

Theoretical models of the phonon thermal conductivity, also based on the Boltzmann's equation, show that phonon thermal conductivity increases with specific heat, phonon group velocity, and phonon relaxation time.[3] Phonon relaxation time can be reduced by scattering of phonons, which can be achieved through appropriate alloying or addition of phonon rattlers.

2.4.2 Fine Grained Materials

Theory suggest that the thermal conductivity of fine grain materials will be reduced by phonon scattering off grain boundaries for materials whose grain size is comparable to or smaller than the phonon's mean free path. At room temperature phonons have a mean free path of approximately 0.3 μm.

Phonons have a wavelength of 1-2 nm at room temperature so they are easily scattered off of grain boundaries with a surface roughness of around 3-5 Å. In contrast, electrons, with a room temperature wavelength of 8 nm at room temperature, will interact with the grain boundaries specularly and are not scattered much at the grain boundary

Phonon scattering also occurs when phonons collide with each other. This is the form of scatter which limits lattice thermal conductivity in bulk materials. Unless the grain size within the material is comparable to or smaller than the phonon mean free path, phonon-phonon scattering will dominate and the thermal conductivity will be the same as that in the bulk. If, however, the grain boundaries are close enough together, phonon-grain boundary scattering will dominate and the thermal conductivity will be reduced.

Parrott [4] presented a theory modeling phonon scattering in sintered, highly disordered semiconductor alloys, specifically SiGe alloys, based on the Klemens-Callaway model of thermal conductivity. He predicted that high frequency phonons would be scattered by point defects in highly disordered alloys and the low frequency phonons with wavelengths on the order of the grain size would be scattered off of the grain boundaries.

Bhandari and Rowe[5] extended Parrott's theories of grain boundary scattering to fine grained PbTe. They predicted a 4-6% decrease in thermal conductivity for PbTe with 1μm grain size compared to the single crystal thermal conductivity and an 11-13% decrease for highly disordered alloys of PbTe. A later study by Rowe and Bhandari[6] predicted a 17% decrease in thermal conductivity for a PbSnTe alloy with 0.25 μm grain size over the single crystal and a 21% decrease in PbGeTe alloys.

However, some existing experimental data for fine grained PbTe does not agree with the theoretical model suggested by Parrott[4] and applied by Bhandari and Rowe[5,6]. Kishimoto and Koyanagi[7] studied sintered n-type PbTe of grain size ranging from 0.74 to 3.65 μm. They found that while the thermal conductivity of the fine grained PbTe decrease with grain size, the electric conductivity also decreased. They attributed the decrease in k to a

decrease in k_e rather than a decrease in k_l. Overall, the ratio σ/k decreased rather than increasing with decreased grain size. Kishimoto and coworkers[8] continued their study to sintered n-type PbTe to grain sizes down to 0.1 μm. They found that the σ/k ratio fell much more drastically with decreasing grain size for grains under 0.5 μm.

2.4.3 Nanostructured Materials

In nanostructured materials, such as quantum dots, quantum wires, and superlattices, quantum effects begin to take a role in the material's electron and phonon transport. Overall, thermoelectric properties of the nanostructured materials can be vastly different from that of bulk properties of its parent materials. Researchers hope that quantum confinement can be utilized to increase the density of states for electrons and, thereby, increase the power factor without adversely affecting the thermal conductivity.

Favorable results have already been seen from thermoelectric materials consisting of superlattices and 2D quantum wells for transport parallel to the film plane. Numerous theories predict enhanced thermoelectric performance for quantum wire arrays as well, but difficulties with oxidation of quantum wires and forming electrically contact with individual wires have prevented any of the predicted enhancements from being experimentally verified.[3]

3.0 Experimental Procedure

To test the overall thermal performance of the nano-sized versus micro-sized samples of PbTe and PbSe the thermal diffusivity, the Seebeck coefficient, and the electrical conductivity had to be measured. From the measured values of the material properties, a *ZT* was calculated. All material properties were measured in MIT's Laboratory for Heat Transfer, using experimental set-ups and procedures designed by Hohyun Lee.

3.1 Material Samples

The samples of PbTe and PbSe were prepared at Boston College by Professor Ren's research group. The samples were made by compressing small particles of thermoelectric material in a hotpress under a pressure of 127 MPa and at a temperature ranging from 750° to 900°C for two to five minutes. Exact processing temperature and pressure for each sample are summarized in Table 1. Appropriately shaped samples could then be cut from the pressed pallet.

For each material, two particle sizes were used to produce samples. The smaller particles were on the order of a nanometer long and the larger particles were of the order of a micrometer long. It is expected that the samples made from nanometer-sized particles would have many more grain boundaries than the samples made from the micrometer-sized particles.

Table 1: Processing parameters for the manufacture of each of the samples

Sample	Hot Press Temp (deg C)	Pressure (Mpa)	Hold Time (min)
PbTe micro 1	750	127	2
PbTe micro 2	825	127	5
PbTe micro 3	750	127	5
PbTe nano 1	750	127	5
PbTe nano 2	800	127	5
PbSe micro 1	850	127	2
PbSe micro 2	900	127	5

3.2 Measurement of Thermal Conductivity

The thermal conductivity was calculated from an experimentally measured thermal diffusivity and literature values for sample density and specific heat. The thermal diffusivity was measured following the method presented by Starr[9] and the modified Angstrom method presented by Sidles and Danielson[10].

Both Starr[9] and Sidles and Danielson[10] modeled their samples as a semi-infinite rod in their derivation of thermal diffusivity. The temperature profile in the samples follows the heat diffusion equation

$$\frac{\partial\theta}{\partial t}+\mu\theta=\alpha\frac{\partial^2\theta}{\partial x^2} \tag{12}$$

for which θ is the temperature difference between the sample and the surrounding environment, μ is the coefficient of heat loss from the sides of the sample, and α is the thermal diffusivity.

A heater, running an AC current, is placed on the top of the sample and the far end of the sample is assumed to be at the same temperature as its surroundings, leading to the boundary conditions

$$\theta(x=0,t)=\theta_0+\theta_1\cos(\omega t) \quad \text{and} \tag{13}$$

$$\theta(x=\infty,t)=0 \tag{14}$$

The temperature at any point along the sample is periodic in time. Therefore, the solution to the temperature can be calculated as a Fourier sum in the form of

$$\theta(x,t)=\sum_{n=0}^{\infty}P_n(x)\cos(n\omega t)+Q_n(x)\sin(n\omega t) \tag{15}$$

Substituting the general form of the solution expressed in Equation 15 into the diffusion equation yields a set of coupled differential equations for the Fourier coefficients P_n and Q_n

$$\alpha\frac{d^2P_n}{dx^2}-\mu P_n=Q_n\omega t \tag{16}$$

$$\alpha\frac{d^2Q_n}{dx^2}-\mu Q_n=-n\omega P_n \tag{17}$$

The solution to the set of equations for P_n and Q_n can be found to be

$$P_n(x)=A_n\exp(-a_n x)\cos(\beta_n x-\varepsilon_n) \tag{18}$$

$$Q_n(x)=A_n\exp(-a_n x)\sin(\beta_n x-\varepsilon_n) \tag{19}$$

where

$$a_n=\left\{\left(\frac{1}{2\alpha}\right)\left[(\mu^2+n^2\omega^2)^{1/2}+\mu\right]\right\}^{1/2} \tag{20}$$

$$\beta_n=\left\{\left(\frac{1}{2\alpha}\right)\left[(\mu^2+n^2\omega^2)^{1/2}-\mu\right]\right\}^{1/2} \tag{21}$$

and where A_n and ε_n are arbitrary constants.

Substituting the forms of the Fourier coefficients found in Equation 18 and 19 back into the general form of the solution, Equation 15, and applying the appropriate boundary conditions yields

$$\theta(x,t) = \theta_0 \exp(-a_0 x) + \theta_1 \exp(-a_1 x)\cos(\omega t - \beta_1 x + \varepsilon_1) \qquad (22)$$

From Equation 22, it is clear that the amplitude of the temperature oscillations decreases with increasing distance from the heater. The amplitude decrement, g, between a distance x_1 and x_2 can be expressed as

$$g = \frac{A_1 \exp(-a_1 x_1)}{A_1 \exp(-a_1 x_2)} = \exp(a_1 (x_2 - x_1)) \qquad (23)$$

From Equation 22, the velocity at which the waves propagate down the sample can also be easily found as

$$v = \frac{\omega}{\beta_1} \qquad (24)$$

or substituting in from Equation 21

$$v = \frac{2\pi}{T}\left\{\frac{2\alpha}{(\mu^2 + \frac{4\pi^2}{T^2})^{1/2} + \mu}\right\}^{1/2} \qquad (25)$$

Since the factor μ is generally unknown, King[11] suggested that μ could be eliminated from the calculation of α by measuring the traveling velocity for two different driving features. The traveling velocity can easily be calculated from observation of the time lag between temperature oscillations a two different distances along the sample as

$$v = \frac{\Delta t}{L} \qquad (26)$$

where Δt is the time lag and L is the distance between the two points.

He presents his formula for thermal diffusivity as

$$\alpha = \frac{1}{4\pi}\left(\frac{T_1^2 T_2^2 v_1^2 v_2^2 (v_1^2 - v_2^2)}{T_2^2 v_2^2 - T_1^2 v_1^2}\right)^{1/2} \qquad (27)$$

where T_1 and T_2 are the periods of the two driving voltages and v_1 and v_2 are the corresponding traveling velocities.

Starr[9] also suggests a method for eliminating the unknown factor μ from the calculations. By measuring the amplitude decrement for two different driving frequencies, the thermal diffusivity could be calculated according to his formula

$$\alpha = \frac{\pi L^2}{T_1 \ln(g_1)\ln(g_2)}\left(\frac{a^2 - b^2}{b^2 - 1}\right) \tag{28}$$

where

$$a = \frac{T_1}{T_2} \quad \text{and} \tag{29}$$

$$b = \frac{\ln(g_2)}{\ln(g_1)} \tag{30}$$

Sidles and Danielson[10] brought together King's and Starr's methods into a calculation for the thermal conductivity, which they termed the modified Angstrom method. By measuring both the time lag and the amplitude decrement, a calculation for the thermal diffusivity can be made using only one driving frequency.

By observing that

$$a_1\beta_1 = \frac{\ln(g)\omega}{Lv} \tag{31}$$

from Equations 23 and 24 and that

$$a_1\beta_1 = \frac{\omega}{2\alpha} \tag{32}$$

from Equations 20 and 21, they were able to formulate the following equation for thermal diffusivity

$$\alpha = \frac{2Lv}{\ln(g)} \tag{33}$$

One of the advantages of measuring the thermal diffusivity of the sample can be seen by examining Equations 27, 28, and 33. Neither the heat flow nor the heat loss coefficient, μ, appears in any of these equations. In general, both of these values can be extremely difficult to measure experimentally. On the other hand, temperature as a function of time is fairly easy to determine in the laboratory. The thermal diffusivity, and consequently the thermal conductivity, can be measured much more cleanly in the lab since the values for the heat flow and heat loss have been eliminated from the equation.

The thermal conductivity, k, of the sample can easily be calculated from the experimentally measured thermal diffusivity, α, as

$$k = \rho C \alpha$$

Where ρ is the density and C is the specific heat.

The thermal diffusivity was measured under high vacuum at a pressure of less than 10^{-5} torr to prevent loss of heat from the sample by natural convection. The sample was mounted upright to a copper mounting plate using silver paste. A pair of K-type thermocouples were attached along the length of the sample using silver paste; one approximately one mm from the top edge and the other approximately five mm further down. The alumel and chromel thermocouple leads where both 3.0 milli-inch in diameter. A ceramic heater was placed on the top surface of the sample with thermal contact putty between the sample surface and the heater to reduce the thermal contact resistance.

The heater was powered with a low frequency AC current by a T.D. SR830 Lock-in Amplifier. The temperatures as a function of time at both of the thermocouples were feed directly into the computer through a National Instruments 1394 A/D converter. A LabView program, written by Hohyun Lee, recorded the temperature over time at both of the thermocouples. An overall schematic of the experimental apparatus used for measuring thermal conductivity is shown in Figure 5.

Measurements of the temperature variation in time at each of the thermocouples were recorded for driving voltages with amplitudes of 1.0, 1.2, 1.4, and 1.6 Volts and with driving frequencies of 5 mHz and 10 mHz.

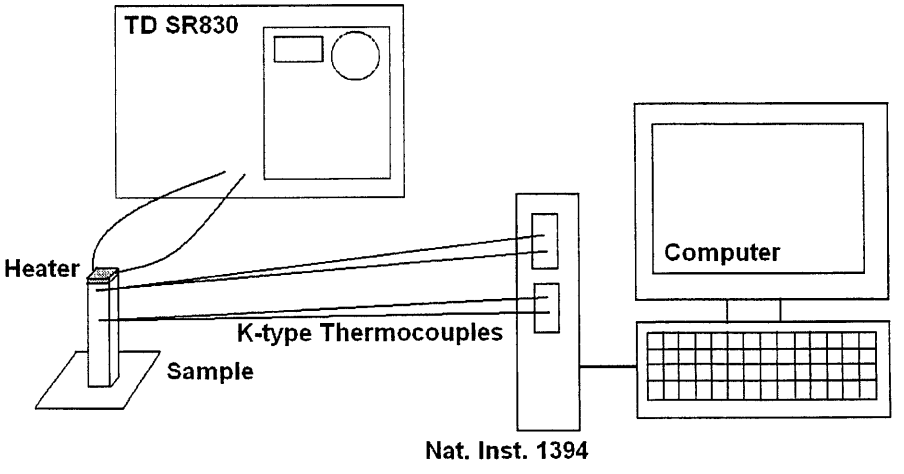

Figure 5: Experimental apparatus for the measuring of the thermal diffusivity.

Data for the temperature curves for each of the driving voltage and frequency pairs was taken to Matlab. In Matlab, a program took the data, guessed an appropriate sinusoidal fit for each of the temperature curves, and used its initial guess to fit a curve to the temperature curve. The program then output a graph of the temperature at the thermocouples plotted with the original data so that the fit could be judged visibly. The Matlab program also outputted the fit parameters for each of the temperature curves. Figure 6 shows a Matlab plot showing the original data for a pair of temperature curves and the calculated fit.

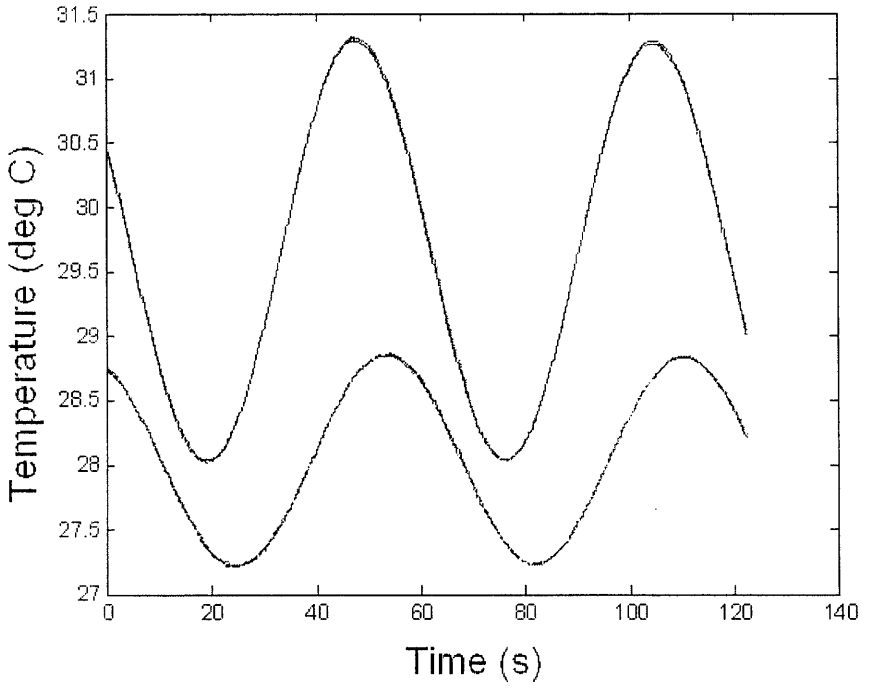

Figure 6: Graphical output of a Matlab program written to calculate the best fit sinusoidal curve for temperature data. These graph shows the original data with the calculated fit for PbTe micro 1 driven at a 1.4 Volt AC current at a frequency of 10mHz

The fit parameters calculated by Matlab were inputted into an Excel spreadsheet where the thermal diffusivity of the sample was calculated according to both Starr's equation and the modified Angstrom method. Table 3 shows the Excel calculations for finding the thermal diffusivity of the sample from the Matlab fit parameters. The spread sheet also calculated the thermal conductivity, k, of the sample from the measure thermal diffusivity and geometric factors according to the formula

$$k = \rho C \alpha \tag{34}$$

where ρ is the density and C is the specific heat.

Table 2:Excel Spreadsheet for calculating the Thermal conductivity based off of the Matlab fit parameters.

	MATLAB fit data							
	Offset (degC)	Ampl (deg C)	Freq (rad/s)	Phase (s)	Gain Decr	Vel (m/s)	Diffusivity (m^2/s)	Conductivity (J/m^2*K)
1000-5 Top	25.74	1.22	0.05	144.68				
1000-5 Bot	24.68	0.54	0.05	153.01				
					0.44	5.39E-04	1.48E-06	1.81
1000-10 Top	25.68	0.71	0.11	20.42				
1000-10 Bot	24.65	0.27	0.11	27.71				
					0.37	6.16E-04	1.40E-06	1.73
1200-5 Top	26.76	1.76	0.05	172.14				
1200-5 Bot	25.18	0.77	0.05	180.54				
					0.44	5.34E-04	1.45E-06	1.79
1200-10 Top	26.79	1.03	0.11	60.35				
1200-10 Bot	25.31	0.38	0.11	67.96				
					0.37	5.89E-04	1.33E-06	1.63
1400-5 Top	28.03	2.40	0.05	110.48				
1400-5 Bot	25.82	1.05	0.05	118.83				
					0.44	5.38E-04	1.46E-06	1.79
1400-10 Top	27.98	1.41	0.11	28.58				
1400-10 Bot	25.77	0.52	0.11	36.06				
					0.37	6.00E-04	1.35E-06	1.67
1600-5 Top	29.41	3.14	0.05	180.12				
1600-5 Bot	26.49	1.37	0.05	188.51				
					0.43	5.35E-04	1.44E-06	1.77
1600-10 Top	29.46	1.84	0.11	61.95				
1600-10 Bot	26.53	0.67	0.11	69.63				
					0.36	5.85E-04	1.30E-06	1.60
					Average Value:		1.40E-06	1.72
					Standard Deviation:		6.65E-08	0.08

3.3 Measurement of Seebeck Coefficient

The apparatus for measuring the Seebeck coefficient was similar to the apparatus for measuring the thermal diffusivity and is shown in Figure 7. The Seebeck coefficient was also measured under high vacuum conditions.

The heater was powered with a DC voltage by a Tektronic PS2510G DC power supply. The steady state temperature at each of the thermocouples was recorded by the computer through a LabView program, written by Hohyun Lee. The steady state voltage drop in the sample between the two thermocouples was calculated from the voltage difference between similar leads off of the two thermocouples as measured by a Keithly 2000

Desktop Multimeter (Keithly DMM), which communicated to the computer through a GPIB connection. The steady state voltage difference was also recorded by the LabView program.

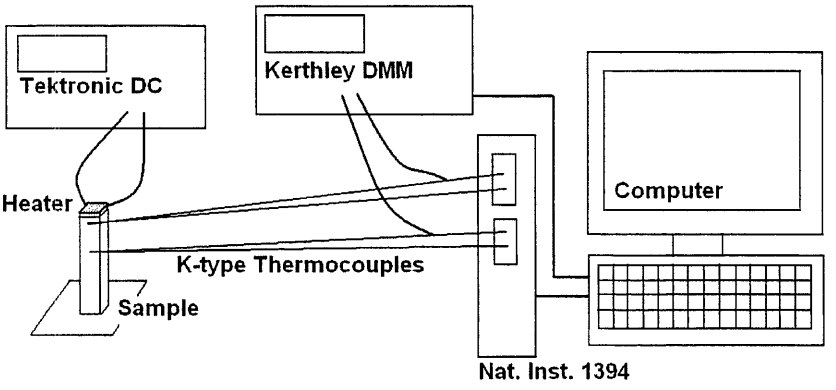

Figure 7: Experimental apparatus for measuring the Seebeck coefficient.

Recalling that the Seebeck coefficient is merely the ratio of voltage difference over the sample to the temperature difference, the Seebeck coefficient is easy to calculate from the graph of voltage drop verses temperature drop.

However, the voltage drop measured by the Keithly DMM does not correspond to the voltage drop over a length of the sample. Since the Keithly DMM is measuring the voltage drop off of a pair of thermocouple leads, it is measuring a voltage that includes both the voltage drop across the sample and the voltage created in the thermocouple leads due to the Seebeck effect in thermoelectric materials subject to a temperature gradient. The total voltage measured by the Keithly DMM will follow the formula

$$V = (T_{amb} - T_h)S_w + (T_h - T_c)S_S + (T_c - T_{amb})S_w \qquad (35)$$

where T_{amb} is the ambient room temperature, T_h is the temperature on the hot side of the sample nearer to the heater, T_c is the temperature of the sample on the cooler end. S_S is the Seebeck coefficient of the sample, and S_w is the Seebeck coefficient of the thermocouple lead wire. Equation 35 simplifies to

$$V = (T_h - T_h)(S_S - S_w) \qquad (36)$$

From equation 36, it is clear that a graph of the voltage as measured by the Keithly verses the temperature drop over the length of the sample will have a slope of $S_S - S_w$, rather than a slope S_S. This can easily be overcome by adding the value of S_w to the measured

slope of the line. Figure 8 shows a typical Seebeck coefficient curve with the measured voltage off of the Keithly DMM plotted against the temperature drop across the sample.

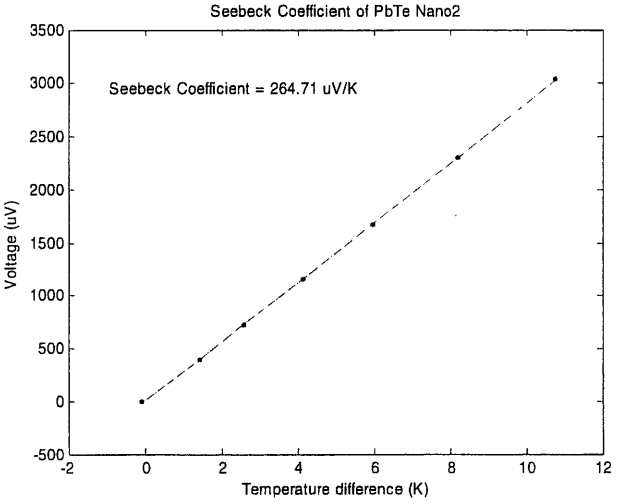

Figure 8: Slope method for calculating the Seebeck coefficient.

3.4 Measurement of Electric Conductivity

The electrical conductivity was measured by placing a sample in a specially designed sample holder, designed and built by Hohyun Lee. The sample rested on two flat plate leads over which a driving voltage could be applied. A HP 33120A function generator supplied an AC driving voltage across the sample and a HP 34410A Desktop Multimeter (HP DMM) recorded the current flowing through the sample. Two thin wire leads, about 1 cm apart, lay across the sample formed the leads to the Keithly DMM that read the voltage drop over a length of the sample. Both the HP DMM and the Keithly DMM exchanged data with a computer through a GPIB connection. The experimental apparatus for measuring the electric conductivity is pictured in Figure 9.

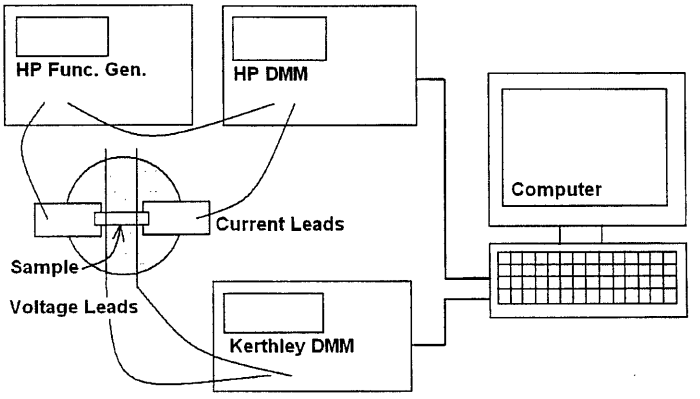

Figure 9: Experimental apparatus for measuring the electrical conductivity.

Voltage drop and current reading were recorded for different driving voltages. The current and voltage measurements were recorded off of the HP DMM and the Keithly DMM by a computer running a LabView program, written by Hohyun Lee. The electric resistivity of the sample was then calculated from the graph of voltage drop versus current and knowledge of the samples geometry.

4.0 Results and Discussion

The samples made with nano-sized grains did not show increased thermoelectric performance over the samples made with micro-sized grains for PbTe and PbSe. The results for the Seebeck coefficient, the electrical conductivity, and the thermal conductivity are summarized in Table 3.

Table 3: Measured properties for each sample and calculated Figure of Merit

Sample	Seebeck Coeff. (uV/K)	Electric Cond. (1/Ohm*m)	Thermal Cond. (W/m*K)	Power Factor	Z (1/K)	ZT at 300K
PbTe micro 1	262.87	1.82E+04	1.77 ± 0.11	1.26E-03	7.11E-04	2.13E-01
PbTe micro 2	216.52	2.56E+04	1.84 ± 0.13	1.20E-03	6.53E-04	1.96E-01
PbTe micro 3		2.78E+04	2.75 ± 0.14			
PbTe nano 1		1.49E+04	1.93 ± 0.13			
PbTe nano 2	264.71	1.55E+04	1.66 ± 0.08	1.08E-03	6.53E-04	1.96E-01
PbSe micro 1	140.82	7.88E+04	1.63 ± 0.10	1.56E-03	9.59E-04	2.88E-01
PbSe micro 2	215.38	3.95E+04	1.55 ± 0.12	1.83E-03	1.18E-03	3.55E-01

4.1 Thermal Conductivity

The thermal conductivity of the PbTe showed only a slight increase with decreasing grain size. The three micro-sized PbTe samples had an average thermal conductivity of 2.12 W/m*K with a standard deviation of 0.45 W/m*K, while the two nano-sized PbTe samples had an average of 1.80 W/m*K and a standard deviation of 0.14 W/m*K. The average of the nano-sized samples showed a 15% decrease from the average of the micro-sized particles. However, given the wide data spread and the small sample size, the average for the nano-sized samples still falls within on standard deviation of the average of the micro-sized.

The two PbSe micro-sized samples had an average thermal conductivity of 1.59 W/m*K with a standard deviation of 0.04 W/m*K.

Theory suggested that materials with grain sizes comparable to the mean free path of the phonon should exhibit lower thermal conductivity due to phonon scattering at the grain boundaries. The expected decrease in thermal conductivity with decreasing grain size was not observed for PbTe or PbSe in this experiment, however.

The lack of a clear decrease in thermal conductivity with decreasing grain size is probably because of grain growth during the hot pressing stage of the sample preparation. The nano- and micro-sized particles are compressed at a pressure of 127 MPa in a hot press at a temperature ranging from 750° to 900°C for up to five minutes. Under these conditions the nano-sized particles will form a material with micro-sized grains rather than nano-sized grains due to grain growth. Likewise, micro-sized particles will form materials with grains that are several orders of magnitude larger than the original micro-sized particles in the hot press.

For the grain boundaries to be effective phonon scatterers, the characteristic length scale of the grains would need to be comparable to the mean free path of the phonons. Otherwise, phonon-phonon collisions become the dominant factor in limiting the lattice thermal conductivity, and the thermal conductivity equals that of the bulk. Grain sizes on the order of 10 μm would not be small enough to be effective at scattering phonons, which have mean free path of approximately 0.3 μm.

To determine if grain growth during the hot pressing stage is truly preventing the observation of a decrease in thermal conductivity, SEM or TEM images of the sample would have to be taken. From a SEM or TEM image, the grain size in the sample material could be observed directly.

4.2 Seebeck Coefficient

A slight increase of 10% was observed in the Seebeck coefficient of the PbTe nano-sized samples in comparison to the micro-sized. The average Seebeck coefficient for two of the micro-sized samples was 239.7 μV/K with a standard deviation of 23.2 μV/K, compared to a measured Seebeck coefficient of 264.7 μV/K for a single nano-size sample. However, the sample size is still extremely small and the distribution of data points is still widespread.

The Seebeck coefficient of one of the nano-sized and one of the micro-sized PbTe could not be measured because of difficulties attaching the two thermocouples to the side of the sample.

4.3 Electrical Conductivity

The electric conductivity of the nano-sized samples of PbTe showed a 34% decrease compared to the micro-sized samples. The electric conductivity of the micro-sized samples was measured to have an average of 23.9 kS/m with a standard deviation of 4.1 kS/m, and the nano-sized were measured to have an average electrical conductivity of 15.2 kS/m with a standard deviation of 0.3 kS/m.

Though the electric conductivity of the nano-sized PbSe sample was measured to be 23% greater than the average electric conductivity of the micro-sized samples, firm conclusions can not be drawn concerning the relation of electric conductivity to grain size due to widespread data points and small sample size.

A slight decrease in the average thermal conductivity of PbTe was accompanied by a clear decrease in electric conductivity. Any decrease in thermal conductivity of the materials can be explained by the decrease in the electric conductivity rather than by phonon scattering. A decrease in electric conductivity would lead to a decrease in electronic thermal conductivity since k_e is proportional to σ.

4.4 Overall Figure of Merit

The overall Figure of Merit for the PbTe and PbSe samples did not change appreciably with grain size. Though the PbTe samples displayed a clear decrease in electric conductivity with decreasing grain size, the influence on the overall Figure of Merit was suppressed by slight decreases in the thermal conductivity, as well.

6.0 Conclusion

The nano-sized samples tested in this study did not yield the hoped for reduction of thermal conductivity for any of the materials tested. No enhancement of thermoelectric performance was seen for the small grain sizes, as classical size effects would suggest.

It is likely that the actual grain sizes in the samples are much larger than their original particle size, for both the nano-sized and the micro-sized particles. Grain growth can occur during the hot press stage of the manufacturing process, yielding materials with grains several orders of magnitude greater than the size of the particles used. If grain growth did occur to this extent, the grain size would have grown too large for phonon-scattering at grain boundaries to be an effective means of lowering the lattice thermal conductivity. A SEM or TEM image of the produced sample is needed to verify whether grain growth occurred. If the grains were able to grow during the hot press stage in the hot press, the processing parameters or the method of production would need to be altered to manufacture samples with reduced thermal conductivity.

References

1 D. D. Pollock: *CRC Handbook of Thermoelectrics*, ed. D.M. Rowe (CRC Press, Florida, 1995) Chap. 1, p.7.
2 G.D. Mahan: *Solid State Physics,* Vol. 51, eds. H. Ehrenreich and F. Spaepen (Academic Press, San Diego, 1997) "Good Thermoelectrics," p.81.
3 G. Chen, M.S. Dresselhaus, G. Dresselhaus, J.-P. Fleurial and T. Caillat: Int. Mat. Reviews, 2003, 48, 1.
4 J.E. Parrot: J. Phys. C. (Solid St. Phys.), 1969, 2, 147.
5 C.M. Bhandari and D.M. Rowe: J. Phys. D (Appl. Phys.), 1983, 16, L75.
6 D.M. Rowe and C.M. Bhandari: Appl. Phys. Lett., 1985, 47, 255.
7 K. Kishimoto and T. Koyanagi: J. Appl. Phys., 2002, 92, 2544.
8 K. Kishimoto, K. Yamamoto and T. Koyanagi: Jpn. J. Appl. Phys., 2003, 42, 501.
9 C. Starr: R.S.I., 1937, 8, 61.
10 P.H. Sidles and G.C. Danielson: J. Appl. Phys., 1954, 25, 58.
11 R.W. King: , , 6, 437.